

MINERALOGICAL CHARACTERIZATION OF SOIL SAMPLES USING X-RAY TECHNIQUES

Mohamed El-Amine OUESSE, Abdou Ciss WADE, Gora DIEYE, Mamoudou SALL, Djibril DIOP

*Laboratory for the Use of X-rays (LUX), Department of Physics, Faculty of Science and Technics
Cheikh Anta Diop University of Dakar - Dakar, Senegal*

omea82@yahoo.fr, abouwade@yahoo.com, dieyegora@gmail.com, basall13@yahoo.fr,
d_diop@yahoo.com

Abstract: This article summarized some characteristics of clayey materials in samples of Senegal such as Thies ENSA, Thies CERAAS, Ndakhar Mbaye and Nioro. Those Four soil profiles situated at different agricultural zones were chosen and soil samples were taken from top and sub-surface layers. The Characterization of Soil samples was performed by different techniques such as X-Ray Diffraction (XRD) and X-Ray Fluorescence (XRF). XRF showed the chemical compositions (major and trace elements) where Al-oxide and silica are present in major quantity. XRD revealed the following soil mineralogical characteristics. The Anatase and Goethite were not detected in Nioro samples. The former constituted the dominant mineral phase while the latter was quantitatively insignificant. The Quartz appears to be more significant in top layers whereas Kaolinite was more abundant in sub-surface layers. This work aims to make a chemical and mineralogical characterizations of soil samples. The idea is to correlate soil minerals composition and the development and growth of crops.

Keywords: X-Ray Fluorescence, X-Ray Diffraction.

1. INTRODUCTION

According to the geological knowledge and the analysis carried out so far, it appears that the soils of Nioro, Thies ENSA, Ndakhar Mbaye and Thies CERAAS analysed in this work are lateritic clays. They would come from a process of laterization of the granites, gneisses and limestones present in the square degrees of Thies ENSA, Ndakhar Mbaye and Thies CERAAS.

These clay soils are predominantly kaolinitic. Indeed, the low cation exchange capacities, the peaks obtained by X-ray diffraction and the absence of swelling are characteristics of the clays of the

kaolinite group. These observations corroborate those of other researchers on tropical soils which have the characteristic of being highly leached and altered.

In addition to kaolinite, the major minerals present in the soils analyzed are quartz, goethite and anatase. Aluminum is almost totally present in kaolinite because we have observed an absence of gibbsite ($\text{Al}(\text{OH})_3$). This absence confirms that the degree of alteration of the soil of the studied region is very advanced. In rough soils, iron is predominantly found in goethite. The goethite generally turns into hematite around 350°C. As for

the anatase, it has a theoretical density of 3.893. Heated above 700°C, it turns into rutile.

The behavior of the soils during an increase in temperature shows two important transformations. The first corresponds to the flow of adsorbed and interfoliar water at temperatures below 150°C. And the second is due to dehydroxylation of the kaolinite between 400°C and 600°C [SG2017]. The transformation of quartz α into quartz β , observed around 573°C, would be important to monitor during baking, as it could lead to cracking.

2. EXPERIMENTAL

All reagents used in this experiment are 99.9% pure. In a typical growth procedure of Y F3 nanospindles composed of nanoplates, YCl_3 (1 mmol), SeO_2 (2 mmol) and NaF (3 mmol) powders were added into 30 ml distilled water and stirred for 2 min. Then the sample was placed in a 40 ml stainless steel autoclave with a Teflon liner, which was maintained at 1008°C for 24 h and then air cooled to room temperature. After reaction, the white precipitate was collected and washed with distilled water and anhydrous alcohol adequately. The final product was dried in a vacuum at 508°C for 4 h.

The obtained samples were characterised by Powder X-Ray Diffraction (PXRD) using a Rigaku D/max-Rapid X-ray diffractometer equipped with a copper anticathode and secondary graphite monochromatised $ICu-K\alpha_{1,2}$ radiation ($\lambda = 1.54178$) [CG1984] and [SG2017].

The identification of the final crystallographic phases was performed by means of X-Ray Diffraction patterns [AS2016] obtained in a step scan automatic diffractometer (Siemens D500) using $CuK\alpha$, as incident radiation and a pyrolytic graphite diffracted-beam monochromator. The investigated angular range was $20^\circ \leq 2\theta \leq 80^\circ$, the angular step was $\Delta 2\theta = 0.04^\circ$ and the counting time per step was $t = 10$ s. The crystal structure refinement was performed with the Rietveld method using a modified version of the DBW 3.9 Young and Wiles program [12] which allows to get accurate analyzes of samples with several phases [13].

Samples were prepared by Metal Organic Chemical Vapor Deposition (MOCVD). Source materials (Toshiba Manufacturing Co. Ltd.) were $Bi(o\text{-tolyl})_3$ and $M(DPM)_2$ with $M = Sr, Ca$ and Cu .

Oxygen was introduced in the reaction tube with a partial pressure of 2.6 kPa and a flow rate of 640 ml/min [DR2016]. X-Ray Diffraction (XRD) measurements were performed on Ultima (Rigaku Co.) and X'Pert MRD (Panalytical Co.) diffractometers ($CuK\alpha$ radiation) [HW2008] and [CJ2016].

3. RESULTS

3.1. X-Ray Fluorescence (XRF) analysis

This technique was used to know the composition of minerals present in samples. The data reported by Table I show silica (SiO_2), alumina (Al_2O_3) and iron oxide (Fe_2O_3) to be present in great quantity while the others are in the form of trace [NG2017].

Table 1. Physical and chemical properties of samples clay soils

Physical and chemical properties	Nioro (20-40) cm	Nioro (140-160) cm	Thies ENSA (140-160) cm	Ndakhar Mbaye (0-20) cm	Thies Ceraas (40-60) m
Oxide	%	%	%	%	%
Na_2O	0	0,077	0,098	0,078	0,069
MgO	0,069	0,072	0,249	0,149	0,215
Al_2O_3	3,365	6,749	17,626	8,905	19,472
SiO_2	92,175	85,067	54,577	80,181	49,008
P_2O_5	0,037	0,027	1,874	1,173	1,979
SO_3	0	0	0,042	0,018	0,36
CaO	0,039	0,094	0,329	0,355	0,214
Fe_2O_3	1,286	1,542	13,884	1,994	17,087
TiO_2	0,511	0,549	1,431	0,741	1,486
K_2O	0,102	0,124	0,313	0,181	0,228
L.O.I.	1,7	3,1	10	4,6	11,2
TOTAL	99,3	97,4	100,4	98,4	101,3

On the other hand the content of Fe_2O_3 is very weak in the 0-20 cm horizon of Ndakar Mbaye. By comparing the concentration of each phase in the various samples one observes a strong content of SiO_2 (80, 181%) in the sample of Ndakar Mbaye. The mass ratio SiO_2/Al_2O_3 [BA2017] is 3,096 for Thies Ensa, 9,004 for Ndakar Mbaye, 2,517 for Ties Ceraas, 12,604 for Nioro 140 - 160 cm and 27,392 for Nioro 20 - 40 cm instead of 1,18 for pure kaolinite. This variation suggests the presence of a significant amount of free silica (quartz, amorphous silica) [NS2003].

The XRF also made it possible to characterize the trace elements contained in the samples. In the Table II, Table III are reported the results obtained and the figure 1, figure 2, figure 3 and figure 4 are interpreted at from results obtained of those samples. These tables and figures reveal the presence of relatively large quantities of Cr, Mn, V, Sr, Zr, Ba, and Ce [LR2014]. Uranium is also detected. It has also revealed an abundance of trace elements in-depth. Indeed, made up mainly of quartz, the soils contain few minerals that might be

able to retain the elements traces in the surface horizon. Thus the high filterability and low reactivity of these soils generate a high risk of migration of the trace elements towards the depth [CD2006]. Essential for the life of plants and animals for some as copper and zinc but potentially toxic for others such as lead or cadmium, the trace elements are either resulting from agricultural, mining and industrial activities of people or are met in a natural state [SD1999].

Table 2: The No1 of trace elements obtained by XRF and their respective concentrations in the samples.

Characteristics	Nioro (20-40) Cm	Nioro (140-160) cm	Thies ENSA (140-160) cm	Ndakhar Mbaye (0-20) cm	Thies Ceraas (40-60) Cm
Elements	Ppm	ppm	ppm	ppm	ppm
Sc	3,7	5,4	22,3	9,6	27
V	22,9	34,8	243,8	44,1	312,1
Cr	28,9	43,5	620,5	121,4	862,2
Mn	303,4	49,1	358,5	175,4	349
Co	4,1	1,7	21,9	6,1	22,2
Ni	7,4	12,6	67,1	19,3	77,8
Cu	2,6	4,8	55,8	12	67,6
Zn	9	13,2	70,3	24,6	71,5
Ga	3,6	7,3	25,9	9,6	29,2
Ge	6,9	7,2	8,1	7,6	7,8
As	nd	nd	0,4	nd	5,5
Se	0,6	1,5	1,7	0,9	3
Br	2,7	3,9	13,3	8	16,5
Rb	14,2	14	29,9	16,5	24,3
Sr	13,3	19,5	638,6	429,1	604,8
Y	13	14,4	76,8	36,7	75,5

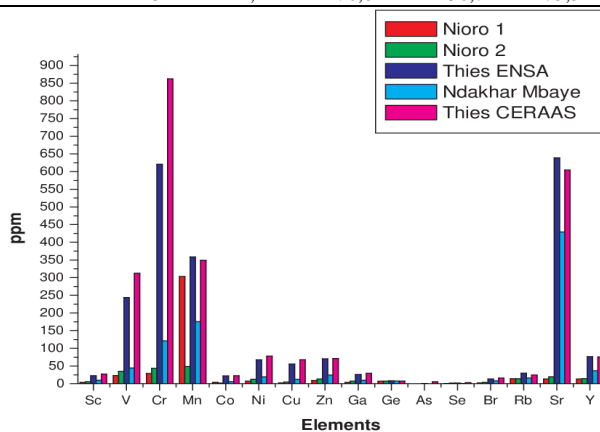


Fig.1. Presentation of the N°1 chemical elements of the samples

3.2. X-ray Diffraction (XRD) analysis

Phases identification

The analysis by X-Ray Diffraction of soil samples (samples without undergone any treatment) provided a series of characteristics diffractogrammes phases present in these samples.

The processing of the diffraction diagrams By Highscore and Jade reveals that they exhibit the lines

characteristic of quartz, kaolinite, anatase and goethite. Figures 5, 6, 7 and 8 report the diffractogrammes of the various samples and their indexation:

The Figure 5 includes the diffractogrammes of the profile of the soil of Ndakhar Mbaye following the various depths 0-20 cms, 20-40 cms, 40-60 cms and 60-80 cms, the values of the indications of Miller (hkl) of the most intense lines are indicated. These diffractogrammes seem quite identical. They mainly show the reflections of the quartz ($2\theta = 50,303; 20,919; 26,796$) and of the kaolinite ($2\theta = 20,103; 25; 12,43$).

We also notice the characteristic peaks of the anatase ($2\theta = 70,218; 83,278; 48,017$) but of weak intensities with regard to the first two phases [DT2017]. In contrast to the others, the diffractogramme of the 60-80 cm horizon indicates the presence of an additional reflection identified by the peak (100) ($2\theta = 22,225$) of the oxide of magnesium, copper and of lithium $\text{Li}_2\text{MgCu}_3\text{O}_{4.25}$.

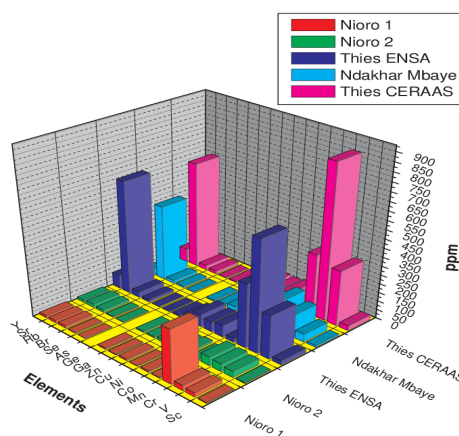


Fig.2. Analysis and comparison of the N°1 of chemical elements of clay samples studied

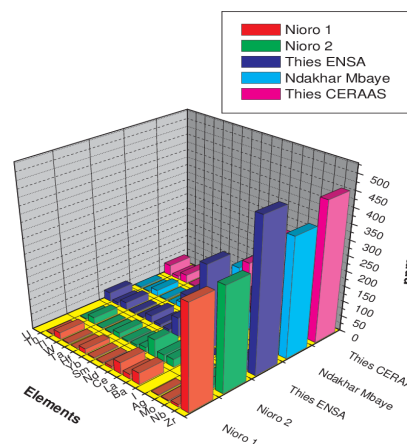


Fig.3. Analysis and comparison of the N°2 of chemical elements of clay samples studied

The figure 7 presents diffractogrammes indexed by horizons 0 - 20, 40 - 60 and 80 - 100 cms of the profile of the soil of Thies Ceraas. The observed peaks also indicate a strong presence of the reflections of quartz ($2\theta = 5,0,3; 20,919; 26,7$)

and kaolinite ($2\theta = 20,103; 50,14; 12,43$). They also show the characteristic peaks of anatase ($2\theta = 38,549; 25,326; 54,874$) and goethite ($2\theta = 34,795; 21,082; 36,59$).

The Figure 8 reports the diffractogrammes indexed of the various horizons (0 - 20, 20 - 40, 40 - 60, 80 - 100 and 140 - 160 cms) of the soil profile of Nioro. The observed peaks indicate the presence of the quartz ($2\theta = 20,9; 26,7; 36,6$) and of the kaolinite ($2\theta = 12,3; 20; 24,9$).

4. DISCUSSION

In the observed horizons, the concentrations in major elements reflect the mineralogy of these soils, which are widely dominated by aluminosilicates (Al_2O_3 and SiO_2).

The highest value of SiO_2 (92,175%) is obtained in the horizon 20 - 40 cm of Nioro. The decrease of this value in-depth in the horizon 140 - 160 cm (85,067%) is due to the strong resistance of the quartz to alteration leading to a low mobilization of the silicon in-depth. Considering the 140-160 cm horizon, the concentration of silicon is greater in the sample Thies Ensa with a value of 54,577% explaining the high value of quartz in the sample Nioro (58,68%) with regard to that obtained with Thies Ensa (9,47%).

For alumina we notice that its variation goes in the opposite direction to that of quartz, i.e. a decrease of quartz results in an increase in alumina. The largest concentration of this element in the 40 - 60 cm horizon of Thies Ensa 19, 472% comparable to that of Thies Ensa 140 - 160 cm (17,626%) is strongly superior to those obtained in the other samples in which horizon 20-40 cm has the lowest rate (3,365%). These two fractions (Si and Al) are involved in soil physicochemical and biochemical processes and could be accumulated by plants.

There is also an accumulation of iron in Thies CERAAS 40-60 cm (17,087%) and Thies ENSA 140-160 cm (13,884%). Indeed, the alteration of primary minerals in the surface horizon releases elements which migrate in soil solution. A fraction of the Al and Fe so dissolved accumulates then in lower horizons.

The distribution of the concentration of P follows that of Al and Fe. P_2O_5 affinity for oxides and hydroxides of Al and Fe is strongly responsible for the suitability of the concentration profiles of Al, Fe and P. The

sodium Na, identified in the form of sodium oxide Na_2O and absent in the upper horizon of Nioro, is very low in all others with comparable proportions 0,077; 0,098; 0,069 and 0,078 % for Nioro 140-160 cm, Thies ENSA 140-160 cm, Thies CERAAS 40-60 cm and Ndakhar Mbaye 0 - 20 cm respectively.

The presence of elements such as Mg, K, Ca, and Fe in samples could be an indicator of the presence of minor quantities of other mineral phases (vermiculite, illite, for instance) that are below the detection limit. Loss on ignition (L.O.I), consist in heating the sample under air and at high temperature to eliminate certain materials depending on the temperature (e.g. humidity) and make reproducible measurements possible in order to be able to compare several samples.

5. CONCLUSION

The main aim of the present work was to determine the mineralogical, physico-chemical and technological features of four clay samples found in areas agricole. The studies undertaken within the framework of this work aimed at the determination of the distribution along the profiles of minerals and chemical elements present in our soil samples. From a mineralogical point of view, the X-ray Diffractometion technique showed the presence of four types of minerals distributed in the various studied profiles:

The anatase constitutes the major phase in the profiles of Ndakhar Mbaye and Ties ENSA soils with a prevalence in the seconds. It is more abundant in-depth. It was not detected in Nioro.

The Quartz is more abundant in top layers' horizons. Its variation along the profiles is irregular except in the soil of Ndakhar Mbaye where it decreases regularly in-depth.

The Kaolinite for its part is more abundant in the lower horizons for the soils of Nioro, Thies ENSA and Thies CERAAS whereas for the profile of Ndakhar Mbaye the great rate is detected in the intermediate horizons 20 - 40 and 40 - 60 cm. The abundance of this mineral is lower in the soil of Thies ENSA.

The goethite is the mineral quantitatively weakest. Its variation along the profiles is irregular. It is relatively more significant in Thies ENSA and almost non-existent in Thies CERAAS. The goethite was not detected in Nioro.

From the elementary point of view, the data obtained in X Ray Fluorescence Spectrometry show a strong concentration of the aluminosilicate grounds. Such a composition confers one to them high content in silicon, element which the cereal plants need to fight

against the cryptogamic diseases and insect bites [BT1994].

6. REFERENCES

- [BA2017] Baghdad Abdelmalek, Bouazi Reikia, Bouftouha Youcef, Bouabsa Lakhdar and Fagel Nathalie; "Mineralogical characterization of Neogene clay areas from the Jijel basin for ceramic purposes (NE Algeria-Africa)"; Applied Clay Science 136; pp 176-183; 2017
- [DT2017] Désiré Tsozué, Aubin Nzeukou Nzeugang, Jacques Richard Mache, Suilabayuy Loweh and Nathalie Fagel; "Mineralogical, physico-chemical and technological characterization of clays from Maroua (Far-North, Cameroon) for use in ceramic bricks production"; Journal of Building Engineering 11; pp 17-24; 2017
- [NG2017] Neli Glavas, Maria Lourdes Mourelle, Carmen P. Gómez, José Luis Legido, Nastja Rogan Smuc, Matej Dolenc and Nives Kovac; "The mineralogical, geochemical, and thermophysical characterization of healing saline mud for use in pelotherapy"; Applied Clay Science 135; pp 119-128; 2017
- [SG2017] Stewart G.Wilson, Jean-Jacques Lambert, Masami Nanzyo and Randy A Dahlgren; " Soil genesis and mineralogy across a volcanic lithosequence"; Geoderma 285; pp 301-312; 2017
- [AS2016] Abdulrahman Shahul Hameed; "Cathodes base de phosphate et anodes composées à base d'oxyde de graphène réduit pour les applications de stockage d'énergie"; Springer Science; Singapore; 2016 [CJ2016] Christopher J. Matocha, John H. Grove, Tasios D. Karathanasis and Martin Vandiviere; "Changes in soil mineralogy due to nitrogen fertilization in an agroecosystem"; Geoderma 263; pp 176-184; 2016
- [DR2016] Dipti Ranjan Biswal, Umesh Chandra Sahoo and Suresh Ranjan Dash; "Characterization of granular lateritic soils as pavement material"; Transportation Geotechnics 6; pp 108-122; 2016
- [LR2014] Leyser Rodrigues Oliveira, Humberto P. Cunha, Nilvânia M. Silva and Ivani P.M. Pádua; "Chemical and Mineralogical Characterization and Soil Reactivity of Brazilian Waste Limestones"; APCBEE Procedia 9; pp 8-12; 2014
- [HW2008] Harris W.G. and White G.N.; "X-ray diffraction techniques for soil mineral identification In: Ulery, A.L., Drees, L. R. (Eds.), Methods of Soil Analysis. Part 5 - Mineralogical Methods". Soil Science Society of America Book Series, Madison, WI, pp. 81-115; 2008
- [CD2006] C. Dère et al., "Reconstitutions des apports en éléments traces métalliques et bilan de leur migration dans un Luvisol sableux soumis à 100 ans d'irrigation massive par des eaux usées brutes," C. R. Geoscience 338; pp 565-573; 2006
- [NS2003] Nibambin Siaka Soro, "Influence des ions de fer sur les transformations thermiques de la kaolinite," Thèse (2003)
- [SD1999] Schulze Darrell et al., "Cristallochimie des éléments traces et devenir des composés minéraux organisés à courte distance dans les sols," Scientific registration No4022; Symposium No22; 1999
- [BT1994] B. T. Cheng, "Le silicium, un élément en tenir compte dans l'étude de la fertilité du sol et de la physiologie des plantes," Bull. Agrosol, Sainte-Foy, Quebec (Canada) 7; pp 55-56 (2); 1994.
- [CG1984] Churchman G.J., Theng B.K.G., Claridge G.G.C. and Theng B.K.G.; "Intercalation method using formamide for differentiating halloysite from kaolinite"; Clay Clay Miner. 32 (4); pp 241-248; 1984